Scanning tunneling microscopy of DNA: Atom-resolved imaging, general observations and possible contrast mechanism

M. G. Youngquist, R. J. Driscoll, T. R. Coley, W. A. Goddard, and J. D. Baldeschwieler
A. A. Noyes Laboratory of Chemical Physics, California Institute of Technology, Pasadena, California 91125

(Received 24 July 1990; accepted 18 September 1990)

We have shown that it is possible to image DNA with atomic resolution using scanning tunneling microscopy (STM), [R. J. Driscoll, M. G. Youngquist, and J. D. Baldeschwieler, Nature **346**, 294 (1990)]. Here we describe that data together with our general observations on STM of DNA in ultrahigh vacuum. We also suggest a possible contrast mechanism for DNA imaging by STM based on wave function orthogonality requirements between a molecule and its substrate. Topographic images are presented which resolve atomic features in addition to the double helical structure and nucleotide pairs of the DNA molecule. Comparisons of experimental STM profiles and modeled contours of the van der Waals surface of *A*-DNA show excellent correlation. Successive scans show that the imaging is nondestructive and reproducible. For this study, double-stranded DNA was deposited on highly oriented pyrolitic graphite without coating, shadowing, or chemical modification.

I. INTRODUCTION

Atomic resolution imaging of individual large biomolecules has been an elusive goal. Using a scanning tunneling microscope (STM) we have been successful in obtaining real-space atom-resolved images of double-helical DNA.[1] This result further demonstrates the potential of the scanning tunneling microscope (STM) for characterization of large biomolecular structures. At the same time, it places tighter constraints on mechanisms which may be proposed to explain STM imaging of such materials. In this paper, we describe our general observations in the imaging of DNA with an STM and suggest a possible contrast mechanism.

The first STM image of DNA (unmodified, under vacuum) was obtained by Binnig and Rohrer[2] in 1984. Other early studies of DNA used metal-shadowing,[3] but recent investigations on DNA in air,[4,5] under water,[6] and under oil,[7] showed that the STM has considerable potential for the study of uncoated biomolecules. Studies on single-stranded DNA[8] suggested that atomic resolution on biostructures is possible. This report provides additional evidence to that end.

II. EXPERIMENT

The sample was a ~550 bp fragment of mouse B-cell V-region DNA.[9] A 2 μl drop of 10 mM aqueous ammonium acetate solution containing 10 ng DNA/μl was deposited on HOPG (Union Carbide zya grade) in air and dried in vacuum. No visible residue was present. Imaging was done on a UHV-STM system which was constructed at Caltech and is similar to the familiar IBM "pocket-size" STM.[10] On semiconductor surfaces, its vertical resolution has been as good as ~1 pm. The system incorporates *in vacuo* tip and sample transfer and has a base pressure of $\sim 3\times 10^{-11}$ Torr. We concurrently obtain topographical (constant current) and gap-modulated "barrier height" images[4] and can perform simultaneous current-voltage spectroscopy (CITS) measurements.[11] Tips were electrochemically etched (6 V ac; 2 M KOH) tungsten without further treatment. Sample bias for the atom-resolved data in this report was + 100 mV with a feedback tunneling current of 1 nA. The z modulation in barrier height measurements was 0.6 Å pp at 1 kHz.

III. RESULTS AND DISCUSSION

A. General observations/discussion

Using this method of sample preparation, predominantly large areas of atomically flat graphite were seen with occasional mono- and biatomic steps. These steps can be mistaken for DNA strands in topographical images,[12] especially if insufficient data-pixel resolution is used. Graphite steps are often linear over hundreds of angstroms and accompanied by similar steps at 60° or 120° to each other. Substrate and DNA structures can usually be distinguished using barrier height information;[13] barrier height changes appear to be much greater over DNA than steps. The $d(\ln i)/ds$ values we measure using the gap modulation technique are often too low to reflect the true barrier height of the surface;[14] however, we find such "barrier height" images to be an indispensable aid in interpreting topographic images. Barrier heights over DNA structures were usually approximately 100–300 meV, but values as high as 1.5 eV were not uncommon. The barrier height over the bare graphite substrate was almost always lower.

The (rarely encountered) DNA structures consisted mainly of large aggregates and clumps. Figure 1 shows a series of three STM topographical images of a typical DNA aggregate; here, a "toroidal" aggregate at increasing magnifications is presented. Although the rear half of the toroid seems to "collapse," the barrier height response is nearly constant around the entire structure. This may be due to spatial differences in the strength of the DNA/substrate interaction.

We have imaged DNA structures using a variety of scan rates and bias voltages. Although our highest resolution images were obtained with very low scan rates (100 Å/s) and + 100 mV sample bias, we do not know whether these parameters are critical. The fundamental requirement is that the scan rate be sufficiently low for the feedback system to respond to > 10 Å changes in topography before the tip has

 0734-211X/91/021304-05$01.00

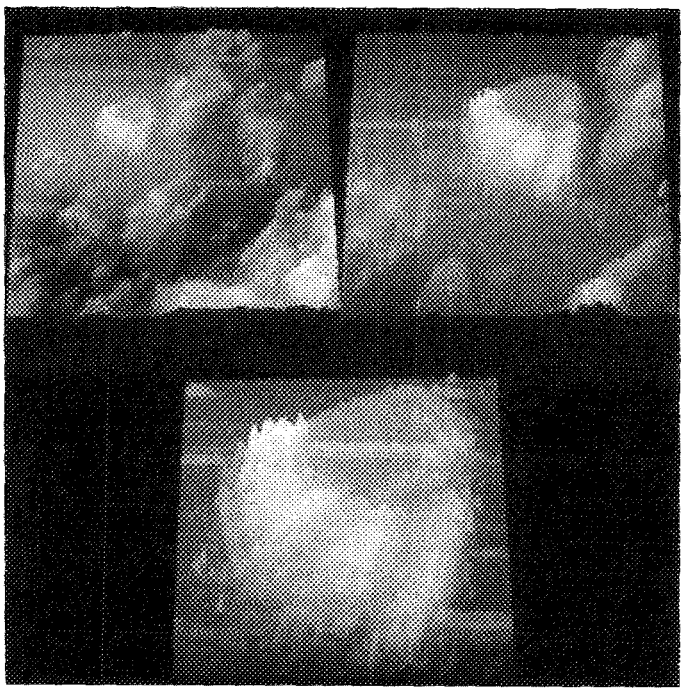

FIG. 1. A series of three topographical images of a toroidally shaped DNA aggregate at successively higher magnification clockwise from top left. Raw data are shown; white corresponds to topographic maxima. The image areas are approximately (3000 Å)^2, (1500 Å)^2, and (750 Å)^2, respectively. The lower right region of the highest magnification image shows several vertical closely packed side-by-side DNA strands with pitch repeats of ~30 Å. Tunnel current 1 nA; sample bias + 200 mV.

moved more than about an angstrom. Images obtained successively with opposite biases are generally indistinguishable and appear qualitatively the same over a range from 50 mV to 1 V.

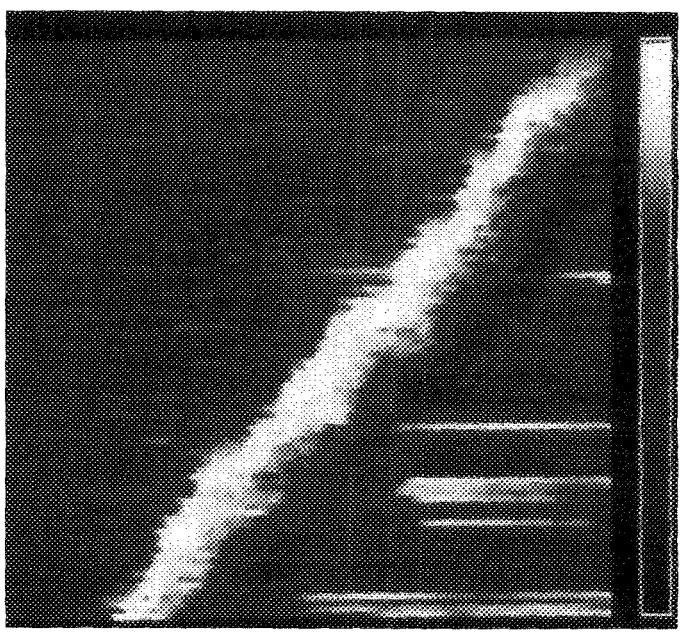

FIG. 2. Unsmoothed, unfiltered plane-subtracted constant-current STM image ~200×200 Å (500×100 data pixels) of an isolated DNA molecule. Nearly eight turns of the helix are shown. The average helix pitch is 30 Å and molecular width 25 Å. A "kink site" with a relative angle of 30° is seen in the middle of the image. Tunnel current 1 nA; sample bias + 100 mV.

While UHV provides a clean experimental environment, it may cause some DNA denaturation.[15] However, there is no evidence of obvious denaturation in our STM images of isolated strands. Any intact DNA is probably in the *A*-DNA conformation which is characteristic at low humidity.

The conventional *A* form of DNA, determined by x-ray crystallography, is characterized by a width of ~23 Å, helical symmetry of 11 base pairs/turn, a + 19° base pair tilt to the helix axis, a 28.5 Å pitch, and an axial nucleotide rise of 2.59 Å.[15] Subtracting the van der Waals radii of the backbone phosphate groups, the major groove is narrow and deep (2.7 and 13.5 Å, respectively) and the minor groove is wide and shallow (11.0 and 2.8 Å).

Figure 2 is a 200 Å×200 Å image of an isolated DNA molecule. The image is neither filtered nor smoothed and shows just over seven turns of the helix. The helix pitch appears somewhat varying but the average pitch is ~30 Å and the molecular width is ~25 Å. The center of the image shows a probable "kink site" with a single turn at an ~30° angle to the helix axis. The middle portion of Fig. 2 was scanned with greater pixel density and is shown in Fig. 3.

B. Atom-resolved imaging

Figure 3 is approximately 80 Å in x and 120 Å in y and was acquired with a scan rate of ~100 Å/s. Again, no filtering or smoothing has been applied to the image. The double helix and the major-minor groove alternation are apparent, as are parallel features spanning the minor grooves at an

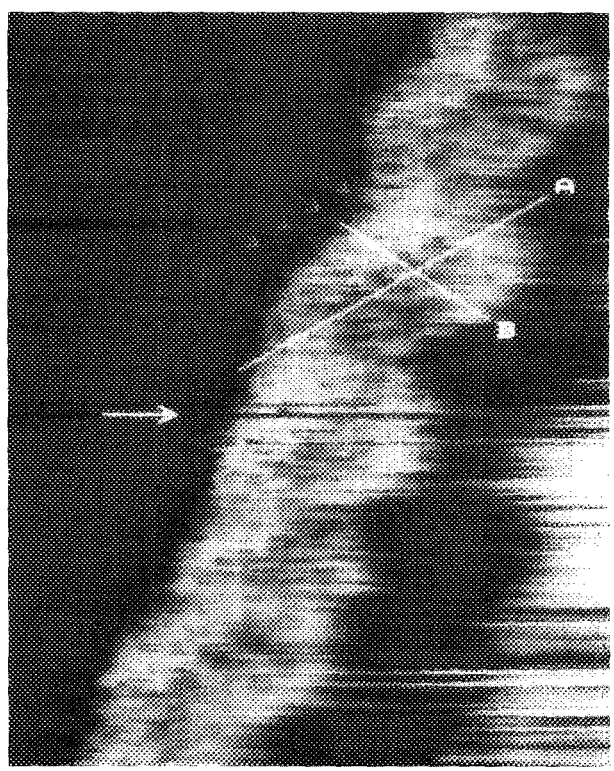

FIG. 3. Plane-subtracted atom-resolved STM image of DNA ~80×120 Å (400×250 data pixels) with no filtering or smoothing. The parallel bands bridging the minor grooves are base pairs at 18° ± 3° to the helix axis. The central arrow points to a tip instability. Tunnel current 1 nA; sample bias + 100 mV. (See Reference 1).

$\sim +18°$ angle to the helix axis. We identify these as the bases of nucleotide pairs. The helix symmetry estimated from these bases is approximately 11 base pairs/turn, consistent with *A*-DNA. The kink site from the previous image is quite evident in this figure and is marked by lines A and B.

The average pitch is ~ 29 Å and the axial nucleotide rise is ~ 2.6 Å, in agreement with the structure of *A*-DNA. These results were surprising to us; we did not expect the STM to faithfully reproduce the van der Waals topography of a DNA molecule. In addition, it was not expected that DNA dried in vacuum on a substrate would have a structure fully consistent with x-ray crystallographic data. The average width of the molecule is ~ 23 Å, and the average "apparent height" is ~ 12 Å. The image acquired scanning in the opposite direction in x shows similar structure, but the molecule appears slightly narrower (~ 21 Å). This may indicate some elastic interaction between the tip and the molecule. The DNA molecule is expected to appear broadened in STM images due to the size and curvature of the tip on the scale of DNA. A shortened "height" of the molecule may be due to dependence of the tunneling probability on both the tip-sample separation and the tunneling barrier. In response to an increased potential barrier over the molecule, the feedback system must reduce tip-sample separation to maintain constant current. The influence of tip structure on images of DNA have also been experienced in which the edge of the tip "senses" the DNA molecule tens of angstroms from the position of the lowest point on the tip. The comparable sizes of the tip and the DNA molecule can lead to an image which is a noticeable convolution of the two structures.

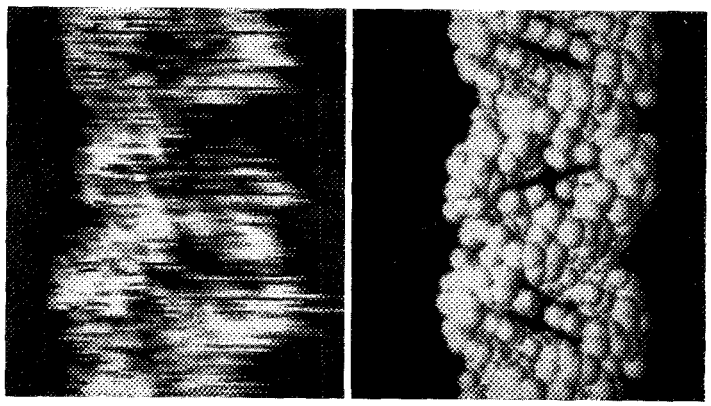

FIG. 5. Comparison of the bottom portion of Fig. 3 with a corresponding section of a van der Waals model of *A*-DNA. The STM data is plane-subtracted and unsmoothed, but contrast has been enhanced by histogram equalization. Hydrogen atoms are omitted from the model for clarity. Model constructed using Biodesign Biograf™ software. (See Reference 1).

Figure 4 is a solid-modeled perspective representation of the bottom three-fourths of Fig. 3. The data have been smoothed using a binomially weighted sliding window average corresponding to a Gaussian of ~ 0.60 Å FWHM (small compared to the typical atomic van der Waals diameter of 3 Å). The bottom third of Fig. 3 is compared to a corresponding section of a van der Waals model in Fig. 5. The y axis is skewed to facilitate direct comparison with the model. The STM image is $\sim 35 \times 55$ Å and contrast has been enhanced by histogram equalization; however, no smoothing has been effected. The same STM data shown in Fig. 5 (without histogram equalization) is compared in Fig. 6 with an identical

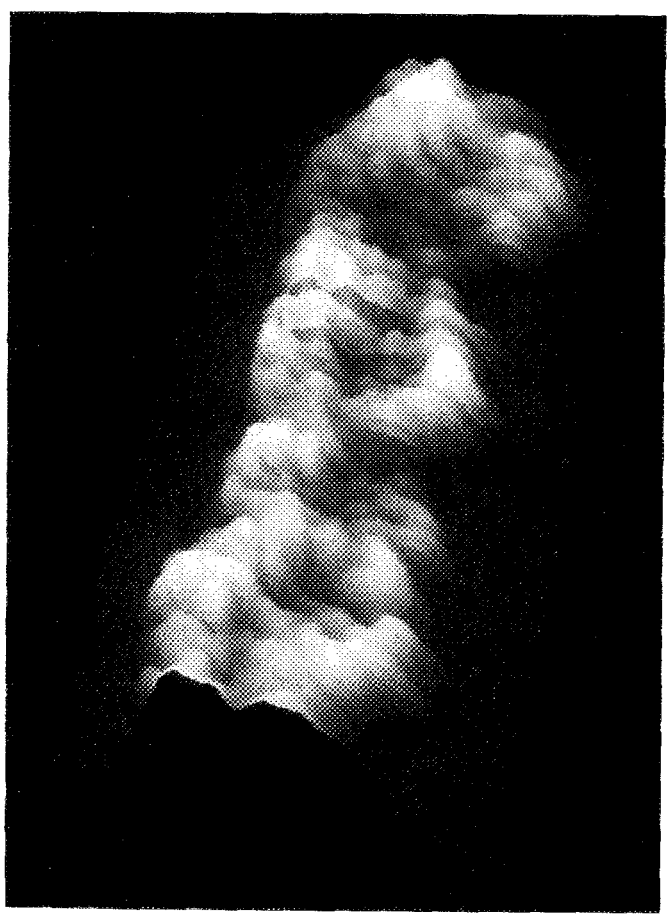

FIG. 4. Solid-modeled perspective representation of the bottom three-fourths of the DNA strand shown in Fig. 3. The image has been smoothed ~ 0.60 Å. The image is $\sim 50 \times 100$ Å. (See Reference 1).

FIG. 6. Comparison of the STM image of Fig. 5 (left) with an STM image of the identical section of the DNA strand obtained ~ 15 min earlier (right). The two images are essentially identical, providing evidence of the nondestructive imaging capabilities of STM. The images are not histogram equalized.

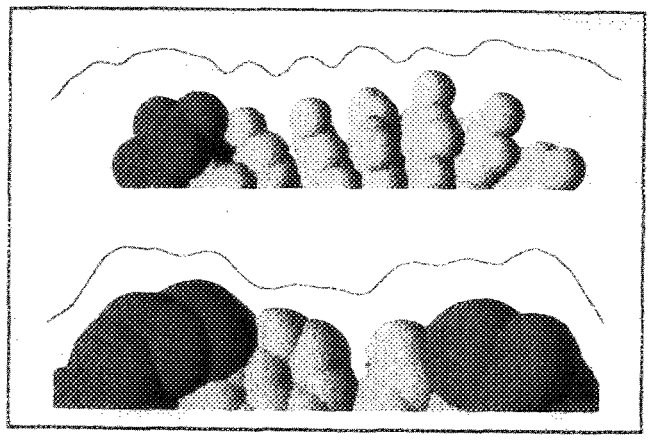

FIG. 7. Interpolated experimental STM tip trajectories following lines marked A and B in Fig. 3 are compared with corresponding atomic contours of an *A*-DNA van der Waals model. The data for line A are shown on top; line B data are on the bottom. Height and length are on the same scale. The data have been smoothed ~0.60 Å. Hydrogens again omitted (See Ref. 1).

section of the DNA strand from an image taken about 15 min earlier. The essentially identical appearance of the two successive images provides evidence of the nondestructive nature of STM imaging even on a large biomolecule like DNA.

In Fig. 7, interpolated cross sections of the STM tip trajectories over the DNA molecule along lines A and B shown in Fig. 3 are compared to the atomic contours of *A*-DNA approximating the cross-sectional regions. These line cuts were chosen to span the minor groove showing the best base pair resolution. In each case, the experimental cross section is placed above the corresponding region of the model. The sugar-phosphate backbone is dark and the base pairs light. The data used for the cuts were also smoothed ~0.60 Å. In the top half of Fig. 7, the cut was taken across the base pair planes, approximating the minor groove axis. Starting at the left, line A cuts through the phosphate-sugar backbone on the leading edge and shows the base pair periodicity across the groove. The cross section in the bottom half of Fig. 7 shows a similar comparison for line B taken across the minor groove through the two high backbones and an intermediate base pair. The nearly atom-for-atom agreement of the cross sections to the contours of the surfaces is highly suggestive of atomic resolution in this region of the image. The ability to resolve surface atoms on a 20-Å-diam "insulating" biomolecule is an extremely interesting result which places a new constraint on proposed imaging mechanisms.

C. Contrast mechanism

The contrast mechanism which permits STM imaging of relatively thick presumably insulating biomolecules like DNA remains poorly understood in the literature. While we recognize that intramolecular conduction pathways may exist in DNA, we know of none consistent with the transport of 10^{10} electrons/sec, the current in our experiments. Furthermore, as Tersoff and Hamann[16] and others have shown, the STM current arises from states near the Fermi level of the sample. In particular, the current accepting states in our experiment must be within 100 meV of the Fermi level. States generated by the strong covalent bonds of a biomolecule composed primarily of second row atoms would be well below (or above) these levels. This suggests the mechanism for tunneling current modulation is only indirectly related to the physisorbed molecule's states.

We propose that the current contrast mechanism arises from an interaction between the adsorbate and graphite substrate which serves only to modulate the underlying bulk states. There are two parts to this interaction, both of which can affect the tunneling current and lead to contrast changes near an adsorbate. The first part of the modulation effect arises from the Pauli principle which effectively requires the orbitals for different bond pairs to be orthogonal. Whereas graphite band states would normally decay exponentially into the vacuum, the presence of the adsorbate interferes with this decay. Orthogonalization of the graphite band states to the orbitals of the adsorbate causes the tail of the band orbitals to rapidly oscillate in the region of the adsorbate and then resume exponential fall-off above the adsorbed molecule. This leads to an extension of the band orbitals to larger distances with the total extent depending on the orientation and character of the molecular orbitals of the interfering molecule. Thus it is plausible that some adsorbate features will be imageable with atomic resolution.

The second part of our contrast mechanism arises from changes in the density of surface states induced by the adsorbate. It is well known that an adsorbate interacting with a surface will have the effect of "pushing" states away from certain energy levels characteristic of the interaction. This has the effect of changing the energy density of states near the interaction. Since the tunneling current is an integral of the product of state-to-state tunneling probabilities and the energy density of states, a contrast will appear physically near the adsorbate. This type of modulation will be most pronounced for strongly interacting adsorbates; thus we expect the first factor (surface state modulation) to be the dominant contrast mechanism for DNA.

Development of a theoretical model to test this hypothesis is in progress. Even without a quantitative understanding of the imaging mechanism, it is clear from the images we and others have obtained that a worthwhile contribution can indeed be made using STM to investigate biological molecules.

D. Future studies

Our results on imaging DNA further demonstrate the great potential of STM for the analysis of biomolecular structures and lend some credence to the idea of using the instrument to sequence DNA. However, the simple DNA deposition method employed in these studies does not yield an even distribution of unaggregated DNA. Additional development is required to make such high-resolution imaging of DNA and similar biomolecular adsorbates commonplace. We are exploring other deposition techniques aimed at minimizing aggregation and providing an even DNA distribution. Electro-spray ionization[17] is one of the more promising methods. Another option under development is the "spreading" deposition of histone-depleted chromosomes as pre-

viously used in electron microscopy (EM) studies.[18] By depleting a chromosome of its DNA-binding histones, it has been shown by transmission electron microscopy (TEM) that one can obtain an even "halo" spread of DNA (diameter $\sim 20\ \mu$) still bound to its central protein scaffold. A modification of EM methods should yield an even and broad distribution of "clean" DNA which would be in a convenient form for routine imaging by STM. Future STM studies include experiments designed to elucidate the imaging mechanism as well as structural characterization of DNA-protein complexes and cruciform DNA structures.

ACKNOWLEDGMENTS

We wish to thank Charles Spence and Joseph Meier of Dr. Leroy Hood's group in the Caltech Biology division for persuading us to undertake this project and for preparing the DNA solution, and Jonathan Hurley and Manish Sud of Biodesign Inc. for molecular modeling software. MGY is a Dept. of Education fellow. This work has been supported by grants from NIH, ONR, Shell Companies Foundation, and the NSF.

[1] R. J. Driscoll, M. G. Youngquist, and J. D. Baldeschwieler, Nature **346**, 294 (1990).
[2] G. Binnig and H. Rohrer, in *Trends in Physics*, edited by J. Janta and J. Pantoflicek (European Physical Society, The Hague, 1984), pp. 38–46.
[3] M. Amrein, A. Stasiak, H. Gross, E. Stoll, and G. Travaglini, Science **240**, 514 (1988).
[4] A. Cricenti, S. Selci, A. C. Felici, R. Generosi, E. Gori, W. Djaczenko, and G. Chiarotti, Science **245**, 1226 (1989).
[5] T. P. Beebe, Jr., T. E. Wilson, D. F. Ogletree, J. E. Katz, R. Balhorn, M. B. Salmeron, and W. J. Siekhaus, Science **243**, 370 (1989).
[6] S. M. Lindsay, T. Thundat, L. Nagahara, U. Knipping, and R. L. Rill, Science **244**, 1063 (1989).
[7] P. G. Arscott, G. Lee, V. A. Bloomfield, and D. F. Evans, Nature **339**, 484 (1989); **346**, 706 (1990).
[8] D. D. Dunlap and C. Bustamante, Nature **342**, 204 (1989).
[9] Ava II fragment of the V_{13} region, from pBV13L cloned by Jerry Siu in Dr. Leroy Hood's research group, Caltech Biology division.
[10] Ch. Gerber, G. Binnig, H. Fuchs, O. Marti, and H. Rohrer, Rev Sci. Instrum. **57**, 221 (1986).
[11] R. M. Tromp, R. J. Hamers, and J. E. Demuth, Science **234**, 304 (1986).
[12] M. Salmeron, T. Beebe, J. Odriozola, T. Wilson, D. F. Ogletree, and W. Siekhaus, J. Vac. Sci. Technol A **8**, 635 (1990).
[13] S. M. Lindsay, EMSA Bull. **19**, 60 (1989).
[14] J. Gómez-Herrero, J. M. Gómez-Rodríquez, R. Garcia, and A. M. Baró, J. Vac. Sci. Technol. A **8**, 445 (1990).
[15] W. Saenger, *Principles of Nucleic Acid Structure* (Springer, New York, 1984).
[16] J. Tersoff and D. R. Hamann, Phys. Rev. Lett. **50**, 1998 (1983).
[17] R. L. Hines, J. Appl. Phys. **37**, 2730 (1966).
[18] J. R. Paulson and U. K. Laemmli, Cell **12**, 817 (1977).